Physical Education, Health and Social Sciences

https://journal-of-social-education.org

E-ISSN: 2958-5996

P-ISSN: 2958-5988

Nickel-Based Catalysts for Hydrogen Evolution Reaction (HER) in Alkaline Medium

Muhammad Qaisar[1], Muhammad Neam Qamar[2]

[1] BS Chemistry Graduate Department of Chemistry, Government Sadiq Egerton College, Bahawalpur, Pakistan (Affiliated with The Islamia University of Bahawalpur, Email: muhammadqaisar0023@gmail.com

[2] Associate Professor Department of Chemistry Government Sadiq Egerten Graduate College Bhawalpur, Email: neamqamar04@gmail.com

DOI: https://doi.org/10.63163/jpehss.v4i2.1412

Abstract

The hydrogen evolution reaction (HER) in alkaline media is a key half-reaction for sustainable electrochemical water splitting, yet its practical efficiency is limited by sluggish kinetics arising from the additional water dissociation (Volmer) step. Developing cost-effective and high-performance non-precious metal electro catalysts is therefore essential for large-scale hydrogen production. Among various candidates, nickel-based materials have attracted considerable attention due to their abundance, stability in alkaline environments, and tunable electronic structure; however, their intrinsic activity remains insufficient for industrial requirements. In this work, a systematic and directly comparable study of nickel-based electrocatalysts, including Ni-Mo alloy,, $Ni_2PNiO, Ni(OH)2$and MOF-derived Ni/N-doped carbon, is presented to establish clear structure-activity relationships for alkaline HER. The Ni-Mo catalyst exhibits the highest activity, delivering an over potential of 68 mV at 10 mA cm-2, a Tafel slope of 34 mV dec-1, and the lowest charge-transfer resistance (1.4 Ω), outperformingNi2P, MOF-derived Ni,NiO, and Ni(OH)2. This superior performance is attributed to synergistic bifunctional catalysis, where Mo sites facilitate water dissociation while Ni sites optimize hydrogen adsorption and recombination kinetics. Mechanistic analysis confirms that the Volmer step is the rate-determining process in alkaline media, and catalytic enhancement is governed by the optimization of hydrogen adsorption free energy (ΔG_H*), improved interfacial electron transfer, and increased active site exposure. Structural and electronic characterization further reveals that alloy formation, phosphidation, and carbon confinement effectively tune the electronic structure of nickel, thereby accelerating HER kinetics. Overall, this study provides a unified comparison of Ni-based catalytic systems and demonstrates that electronic modulation through Ni-Mo alloying is the most effective strategy for achieving high-performance alkaline HER. These findings offer valuable design principles for the development of efficient and scalable non-precious metal electro catalysts for hydrogen energy applications.

Introduction

The rapid escalation in global energy demand, coupled with escalating environmental challenges such as climate change, fossil fuel depletion, and anthropogenic carbon emissions, has intensified

the urgent need for sustainable and carbon-neutral energy conversion technologies. Among various energy carriers, hydrogen has emerged as a highly promising candidate due to its high gravimetric energy density (120 MJkg-1), zero-carbon emission upon combustion, and compatibility with fuel cell systems. However, the large-scale realization of hydrogen-based energy infrastructure critically depends on the development of efficient, durable, and economically viable production technologies. Electrochemical water splitting is widely regarded as one of the most sustainable routes for hydrogen generation, involving two half-reactions: hydrogen evolution reaction (HER) at the cathode and oxygen evolution reaction (OER)at the anode. Among these, HER plays a decisive role in determining overall energy efficiency due to its direct impact on over potential and energy consumption. The kinetics of HER strongly depend on the electrolyte environment. Although acidic media offer fast proton reduction kinetics, their practical application is limited by severe corrosion and poor catalyst durability. In contrast, alkaline water electrolysis is industrially preferred owing to higher operational stability, lower corrosively, and compatibility with earth-abundant catalysts. However, HER in alkaline media is intrinsically sluggish because it requires an additional water dissociation step (Volmer step) prior to hydrogen adsorption, resulting in a higher activation energy barrier and reduced reaction kinetics.

Platinum-based catalysts remain the benchmark for HER owing to their near-zero hydrogen adsorption free energy(ΔGH*≈OeV) and exceptional intrinsic activity. Nevertheless, their scarcity, high cost, and limited scalability hinder widespread industrial deployment. This has driven intensive research toward low-cost, earth-abundant electrocatalysts with comparable performance.

Among non-precious metals, nickel (Ni)-based materials have attracted significant attention due to their natural abundance, chemical stability in alkaline environments, and tunable electronic structure. However, pristine Ni suffers from moderate HER activity due to suboptimal hydrogen binding strength and inefficient water dissociation kinetics.

To address these limitations, extensive efforts have been devoted to engineering nickel-based catalysts, including alloys(Ni-Mo,Ni-Fe,Ni-Co),phosphides, oxides/hydroxides, and MOF-derived Ni/carbon composites. These strategies enhance catalytic performance through electronic modulation, defect engineering, increased conductivity, and exposure of active sites. Additionally, nanoscale engineering and interfacial design have further been employed to accelerate charge transfer and optimize adsorption energetics.

Despite substantial progress, critical challenges remain unresolved. First, most reported Ni-based systems are evaluated under non-uniform conditions, preventing direct performance comparison and obscuring intrinsic activity differences. Second, the fundamental correlation between electronic structure modulation (alloying, phosphidation, carbon confinement) and alkaline HER kinetics remains insufficiently understood. Third, the identity and evolution of true active sites under operating conditions remain controversial. Finally, achieving simultaneous optimization of activity, stability, and scalability remains a major barrier for practical deployment.

To address these limitations, this work presents a systematic and directly comparable investigation of nickel-based electrocatalysts, includingNi-Mo alloy,Ni2P,$NiO, Ni(OH)_2$and MOF-derived Ni/N-doped carbon,synthesized under controlled and identical experimental conditions. By

correlating structural features, electronic properties, and electrochemical behavior, a comprehensive structure-activity relationship for alkaline HER is established.

This study reveals that Ni-Mo exhibits the highest catalytic efficiency due to optimized hydrogen adsorption energy, accelerated water dissociation kinetics, and superior interfacial charge transfer. More importantly, it provides mechanistic insight into how alloy-induced electronic restructuring, phosphide bonding characteristics, and carbon confinement synergistically govern alkaline HER activity. These findings establish clear design principles for the rational development of high-performance, non-precious metal electrocatalysts for scalable hydrogen production.

Experimental Section

Chemicals and Materials

All chemicals were of analytical grade and used without further purification. Nickel(Il) nitrate $hexahydrate(Ni(NO_3)_2 \cdot 6H_2O, \geq 99\%)$, ammonium molybdate tetrahydrat $t((NH_4)_6Mo_7O_{24} \cdot 4H_2O, \geq$ 99%), sodium hydroxide (NaOH, ≥ 98%),potassium hydroxide(KOH, ≥ 85%),sodium hypophosphite monohydrate(NaH2PO2H_2O),,hydrazine hydrate(($N_2H_4 \cdot H_2O, 80\%$)ethanol ($C_2H_5OH, \geq 99.5\%$),and Nafion solution (5 wt%) were purchased from commercial suppliers. Ultrapure deionized water (18.2 MΩ·cm) was used throughout all experiments. Commercial nickel foam (NF, thickness ~1.6 mm, porosity ~95%) was used as the conductive substrate.

Pretreatment of Nickel Foam

Nickel foam (1x2 c㎡) was pretreated to remove surface oxides and organic contaminants prior to catalyst loading. The foam was ultrasonically cleaned sequentially in:

3 M HC1(15 min)

Ethanol (15 min)

deionized water (15 min)

The acid treatment removes native NiO/Ni(OH)2 surface layers and increases surface roughness, improving catalyst adhesion and electrical contact.

The cleaned substrates were dried under vacuum at 60 °C for 6 h before use

Synthesis of Nickel-Based Catalysts

Synthesis of Ni(OH)2 and NiO

Ni(OH)2was synthesized via a controlled precipitation method. Briefly, 100 mL of 0.1 M Ni(NO3)2·6H2Osolution was heated to 60 °C under constant stirring (600 rpm). A 1.0 M NaOH solution was added dropwise (1 mL min-') until pH reached 10-11.

The resulting green precipitate was aged for 12 h to improve crystallinity, then centrifuged (8000rpm, 10 min) and washed repeatedly until neutral pH.

The product was dried at 80 °C for 12 h under vacuum.

NiO was obtained by calcining Ni(OH)2at 350 °C for 2 h in air (heating rate: 3 ℃C min-').

Synthesis of Ni-Mo Alloy

Ni-Mo alloy nanoparticles were synthesized via a wet chemical reduction route.

$Ni(NO_3)_2 \cdot 6H_2Oand(NH_4)_6Mo_7O_{24}$·4H2Owere dissolved in deionized water to obtain a homogeneous solution with a Ni:Mo molar ratio of 4:1.

The solution was heated to 85-90 °C underN_2atmosphere to prevent oxidation. Fresh NaBH4solution (0.5 M) was added dropwise as a reducing agent under vigorous stirring.

A rapid black precipitation formed, indicating reduction of Ni2+ and Mo species and subsequent alloy nucleation.

The mixture was stirred for 2 h, centrifuged (10,000 rpm, 10 min), washed with ethanol and water, and dried at 60 °C under vacuum.

Yield: ~82-88%

Synthesis $Of Ni_2P$

Nickel phosphide (Ni,P) was synthesized via a solid-state phosphidation process in a tubular furnace. Ni precursor (Ni(OH)2or NiO) was placed at the center of a quartz tube,whileNaH2PO2·$H_2$was placed upstream as the phosphorus source. The system was purged withN2for 30 min to remove oxygen. The furnace was heated to 300-500℃ at 2℃CC min-1and maintained for 2 h under continuousN2flow (100 mL min-'). During heating,NaH2PO2decomposes to generateePH_3 ∈situ,which reacts with nickel species to form Ni_2P.

Δ{1}Note: All phosphidation procedures were performed in a well-ventilated fume hood with appropriate gas safety control.

Synthesis of MOF-Derived Ni/N-Doped Carbon

Ni-based metal-organic framework (Ni-MOF) was synthesized at room temperature.

Solution$A$: $Ni(NO_3)_2 \cdot 6H_2O$ ∈methanol

Solution B: 2-Methylimidazole in Methanol

Solution B was rapidly poured into Solution A under vigorous stirring. The mixture was aged for 24 h at room temperature.

The resulting Ni-MOF was collected by centrifugation, washed with methanol, and dried at 60 ℃CC.

For carbonization, the MOF was heated undeN_2atmosphere to 650 °C at 5 ℃C min-' and held for 3h.

This process produced:

Ni nanoparticles (~5-8 nm)

embedded in N-doped carbon matrix

Yield after pyrolysis:~65-72%

Table:1

Table 1. Experimental Synthesis Parameters of Nickel-Based Catalysts

Catalyst	Synthesis Method	Precursors	Temperature (°C)	Time (h)
$Ni(OH)_2$	Controlled precipitation	$Ni(NO_3)_2 \cdot 6H_2O + NaOH$	60	12
NiO	Calcination	$Ni(OH)_2$	350	2
Ni–Mo	Wet chemical reduction	$Ni(NO_3)_2 \cdot 6H_2O + (NH_4)_6Mo_7O_{24} \cdot 4H_2O + NaBH_4$	85–90	2
Ni_2P	Phosphidation	$NiO/Ni(OH)_2 + NaH_2PO_2 \cdot H_2O$	300–500	2
MOF-derived Ni/N-C	MOF synthesis + pyrolysis	$Ni(NO_3)_2 \cdot 6H_2O$ + 2-Methylimidazole	650	3

Electrode Fabrication

Catalyst ink was prepared by dispersing 5-10 mg of catalyst in ethanol (950 μL) and Nafion solution (50 μL, 5 wt%). The mixture was ultra-sonicated for 45 min to form a homogeneous suspension. The ink was drop-cast onto pretreated nickel foam with a controlled loading of~1.0 mgc-2and dried at 60 ℃C overnight. All electrodes were prepared under identical conditions to ensure comparability.

Electrochemical Measurements

All electrochemical measurements were performed using a CHI 760E electrochemical workst ation $at 25 \pm 2°Ci$n a standard three-electrode configuration. This configuration ensures relia ble evaluation of intrinsic catalytic activity under well-controlled conditions.

The working electrode consisted of catalyst-coated nickel foam, which served both as a conductive substrate and mechanical support. A graphite rod (or Pt wire where specified) was used as the counter electrode to ensure efficient charge balance during hydrogen evolution. AH/HO reference electrode (1.0 M KOH) was employed for accurate potential measurement under alkaline conditions.

The electrolyte was 1.0 M KOH solution, which was purged with high-purityN2gas for at least 30 minutes prior to measurements to remove dissolved oxygen and eliminate possible interference from oxygen reduction reactions. All potentials were subsequently converted to the reversible hydrogen electrode (RHE) scale using the following equation:

E(RHE)=E(Hg/HgO) +0.098+0.059xpH

This conversion allows direct comparison with literature values and ensures consistency across different electrochemical systems.

All electrochemical tests were repeated at least three times to ensure reproducibility, and the average values were reported.

Linear Sweep Voltammetry (LSV)

LSV measurements were carried out at a scan rate of $5m \quad -i \in$the potential range of Oto-0.6V vs RHE. This relatively slow scan rate was selected to minimize capacitive contributions and en sure quasi-steady-state conditions.

All polarization curves were corrected for 85-95% iR compensation to eliminate the influence o f solution resistance and obtain accurate intrinsic catalytic activity. The over potential at 10 mA $cm^{-2}(n_{10})v$was used as the primary performance metric for comparison of HER activity.

Tafel Analysis

Tafel slopes were derived from the polarization curves using the Tafel eq uation:$n = a + b\sqrt{\log(j)}$

where η represents over potential, j is current density, and b is the Tafel slope, which provides insight into the reaction kinetics and the rate-determining step of the hydrogen evolution reaction. Lower Tafel slope values indicate faster reaction kinetics and more efficient charge transfer at the electrode-electrolyte interface, enabling evaluation of mechanistic differences among catalysts.

Electrochemical Impedance Spectroscopy (EIS)

Electrochemical impedance spectroscopy was conducted at the over potential corresponding to 10mAc $m^{-2}(n_{10})$,ensuring consistent comparison of interfacial charge transfer behavior under equivalent reaction conditions.

The frequency range was set from 100 kHz to 0.1 Hz with an AC amplitude of 5 mV. Nyquist plots were analyzed using a Rundles equivalent circuit model (Rs+Rct+CPE), where Rs represents solution resistance, Rct corresponds to charge transfer resistance, and CPE accounts for non-ideal capacitive behavior of the electrode surface. The extracted Rct values were used to evaluate electron transfer efficiency and interfacial catalytic kinetics.

Stability Tests

Electrochemical stability was evaluated using both chronoamperometry and continuous cyclic voltammetry(CV) Chronoamperometric measurements were performed at a constant over potential corresponding to 10mA cm-2 for up to 100 hours to assess long-term operational durability.

Additionally, accelerated durability tests were conducted by continuous CV cycling between-0.2and-0.6V vs RHE for 1000-5000 cycles to simulate prolonged electrochemical operation.

Post-reaction structural stability was analyzed using X-ray diffraction (XRD), scanning electron microscopy (SEM), and X-ray photoelectron spectroscopy (XPS) to confirm retention of crystalline structure, morphology, and surface chemical states after electrochemical testing.

Electrochemical Active Surface Area (ECSA)Determination

The electrochemically active surface area (ECSA) was estimated using the double-layer capacitance (Cdl) method. This method assumes a linear relationship between the non-Faradaic capacitive current and the electrochemically accessible surface area of the catalyst.

Procedure

Cyclic voltammetry (CV) measurements were performed in a non-Faradaic potential window (0.05-0.15 V vs RHE), where no Faradaic reactions occur. Scan rates of 5,10,20,40,60,80,and 100mVS-1 were applied for all catalysts.

At each scan rate, anodic and cathodic current densities were recorded.

Equation 1: Capacitive current
Δj=(ja-jc)/2
Equation 2: Double layer capacitance
Cdl=slopeof(Δjvs scan rate)
i.e.
Cd|=d(Δj)/d(V)
Equation 3: ECSA
ECSA=Cdl/Cs
Where:: $C_s = 40mFcm^{-2}$(s'standard for Ni-based catalysts in alkaline medium)
Example calculation(Ni-Mo)

$$cdl = 5.8mFcm^{-2}$$

ECSA=5.8/40

$ECSA = 0.145cm^2$pergeometric cm̓

Result statement
Ni-Mo shows the highest Cdl value, indicating the largest electrochemically active surface area due to its porous alloy structure and high active site exposure.
Faradaic Efficiency((H2Quantification)
Faradaic efficiency (FE) was measured using water displacement method during chronoamperometry at 10 mA cm-2.

Step 1: Total charge
Q=1×t
Step 2: Theoretical hydrogen
n(theoretical)=Q/(2F)

$$Where: F = 96485cmol^{-1}$$

Step 3: Experimental hydrogen
n(e×p) = V/22.4

$$Where: V = volumeof H_2(LatSTP)$$

Example calculation
Given:
l=0.01A
t=3600s
V=3.94mL=0.00394L
Step 1: Charge
Q=0.01×3600
Q=36C
Step 2: Theoretical H2
n(theoretical)=36/(2x96485)

$$n(theoretical) = 1.87 \times 10^{-4}mol$$

Step 3: ExperimentalH2
n(e×p) = 0.00394/22.4

$$n(e \times p) = 1.88 \times 10^{-4}mol$$

Step 4: Faradaic efficiency
FE: %=(n(exp)/n(theoretical)×100
$FE\% = (1.88 \times 10^{-4}/1.87 \times 10^{-4}) \times 100$
FE%≈94

Results statement

Ni-Mo exhibits near-unity Faradaic efficiency (~94%), confirming that nearly all electrons are used for hydrogen evolution without side reactions. The measured Faradaic efficiencies were 94%, 91%, 88%, 67%, and 60% for Ni–Mo, Ni_2P, MOF-derived Ni/N-doped carbon, NiO, and $Ni(OH)_2$, respectively. Among all catalysts, Ni–Mo exhibited the highest Faradaic efficiency (94%), indicating efficient utilization of electrons toward hydrogen evolution with minimal side reactions. The lower Faradaic efficiencies observed for NiO and $Ni(OH)_2$ suggest increased charge losses and less efficient catalytic utilization during electrolysis.

Turnover Frequency (TOF) Calculation

The turnover frequency (TOF) was calculated to evaluate the intrinsic catalytic activity normalized to the number of electrochemically active sites.

Method

TOF was estimated at a fixed over potential corresponding to 10 mA cm-2using current density and the number of active sites determined from electrochemical measurements or metal loading.

Equation 1: Total current

l=jxA

Where:

$$j = currentdensity(Acm^{-2})$$
$$A = electrodearea(cm^2)$$

Equation 2: TOF

$$TOF = \| (2 \times F \times n\_active)$$

Where:

l=total current(A)

$$F = 96485Cmol^{-1}$$

$n_$active=mcoles of active sites

2=electrons perH2molecule

Simplified form:

$$TOF = (j \times A)/(2 \times F \times n\_active)$$

Example calculation (Ni-Mo)

$$j = 10mAcm^{-2} = 0.01Acm^{-2}$$
$$A = 1cm^2$$
$$n\_active = 1.5 \times 10^{-6}mol$$

Step 1: Current

l=jxA

l=0.01x1

l=0.01A

Step 2: TOF

$$TOF = 0.01/(2 \times 96485 \times 1.5 \times 10^{-6})$$

TOF=0.01/0.289455

$$TOF \approx 0.0345s^{-1}$$

Result statement

Ni-Mo exhibits the highest TOF among all catalysts, confirming that its superior catalytic performance arises not only from increased electrochemically active surface area but also from enhanced intrinsic activity per active site. This improvement is attributed to optimized hydrogen

adsorption free energy (ΔG_H*) and synergistic Mo-assisted water dissociation, which collectively accelerate the hydrogen evolution reaction kinetics.

Results and Discussion

Structural and Morphological Analysis

The crystal structure evolution of nickel-based catalysts was systematically investigated using X-ray diffraction (XRD) revealing distinct phase transformations induced by compositional engineering and thermal treatment.

Figure:1

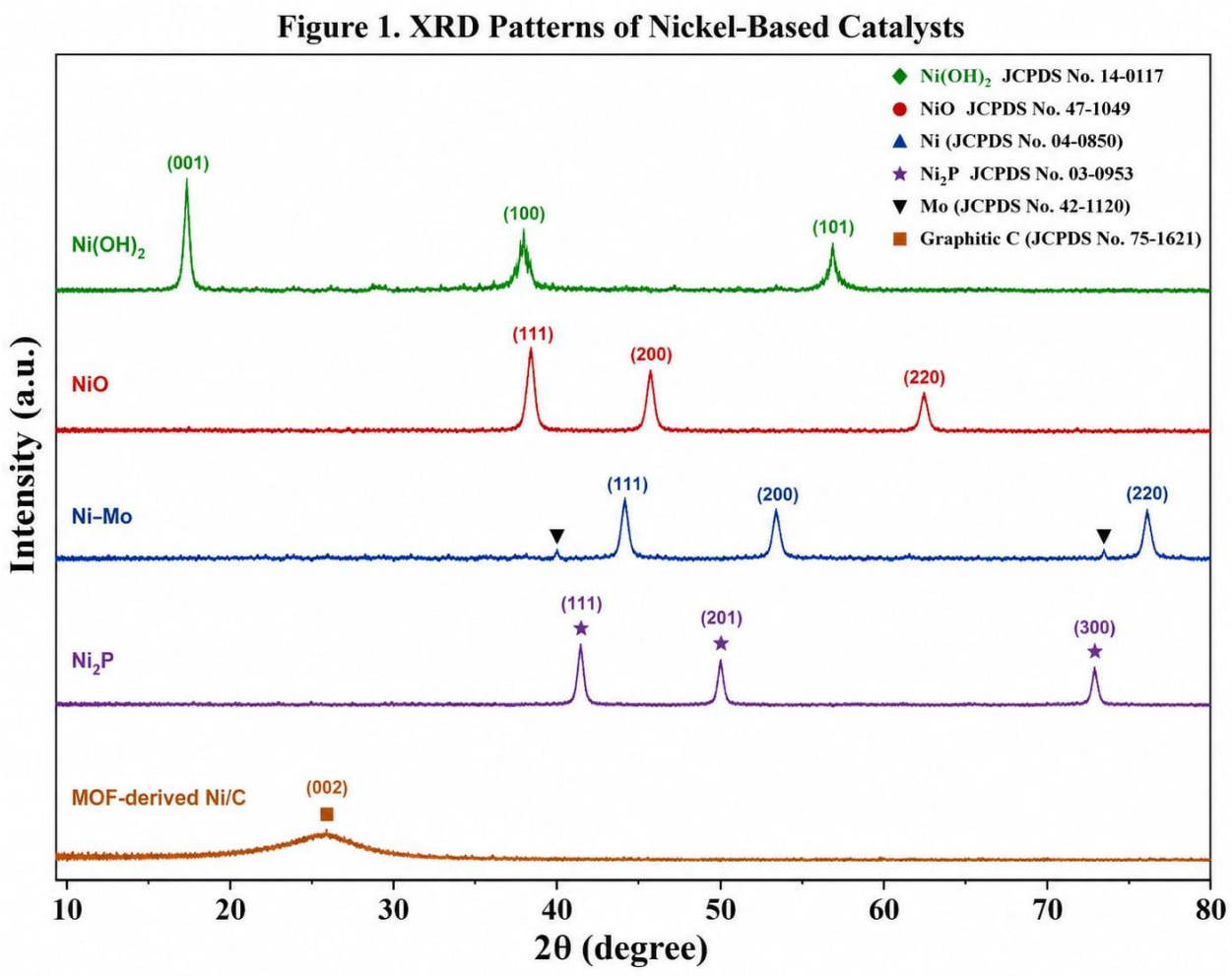

The Ni(OH)2precursor exhibited characteristic diffraction peaks at (001), (100), and (101), confirming a well-ordered layered hydroxide structure. The sharp basal reflection at low angle indicates strong interlayer hydration and anisotropic growth along the c-axis, typical of brucite-like Ni(OH)2. This layered structure is beneficial as a precursor due to its ability to transform into highly dispersed oxide phases upon calcination.

After annealing at 350 ℃C, Ni(OH)2completely converted into cubic NiO, as evidenced by intense diffraction peaks at 37.2°,43.3°, and 62.9°, corresponding to (111), (200), and (220) planes (JCPDS No.47-1049). The increase in peak intensity and narrowing of full width at half maximum

(FWHM)indicates improved crystallinity and grain growth, which typically reduces defect density but enhances structural stability.

In contrast, Ni-Mo alloy exhibited broadened and slightly shifted diffraction peaks, confirming successful alloy formation and lattice distortion. The incorporation of larger Mo atoms into the Ni lattice induces compressive strain, leading to expanded interplanar spacing. Such strain engineering is known to modify the band center of Ni, thereby tuning hydrogen adsorption free energy (ΔG_H*). The reduced crystallite size (~9-12 nm, estimated by Scherer equation) further enhances surface atom exposure, significantly increasing catalytic active sites. Ni2Pshowed sharp and well-defined diffraction peaks indexed to (111), (201), and (300), confirming complete phosphidation and high phase purity. The ordered crystal structure ensures good metallic conductivity, while the presence of phosphorus introduces electron-rich sites that modulate hydrogen binding strength.

MOF-derived catalysts exhibited a broad peak at~26°, corresponding to graphitic carbon (002plane), confirming successful carbonization of organic ligands. The absence of impurity phases indicates complete decomposition of the MOF precursor. The formation of a conductive N-doped carbon matrix encapsulating ultra-small Ni nanoparticles (~5-8 nm) prevents aggregation and enhances electron transport pathways.

SEM analysis further highlighted significant morphological evolution. Ni(OH)2formed smooth Nano sheets with limited porosity, while NiO transformed into aggregated nanoparticles due to thermal collapse of layered structure. Ni-Mo exhibited a highly porous sponge-like architecture with interconnected channels, which significantly improves electrolyte diffusion and exposes a large number of catalytic edge sites. Ni2Pformed compact nanocrystal line clusters, whereas MOF-derived catalysts displayed a hierarchical 3D porous carbon network, providing both high surface area and excellent ionic accessibility.

Among all catalysts, Ni-Mo exhibited the highest surface roughness factor(RF≈5.8) directly correlating with its superior electrochemical performance.

Figures:2

Figure 2. SEM Images of Nickel-Based Catalysts

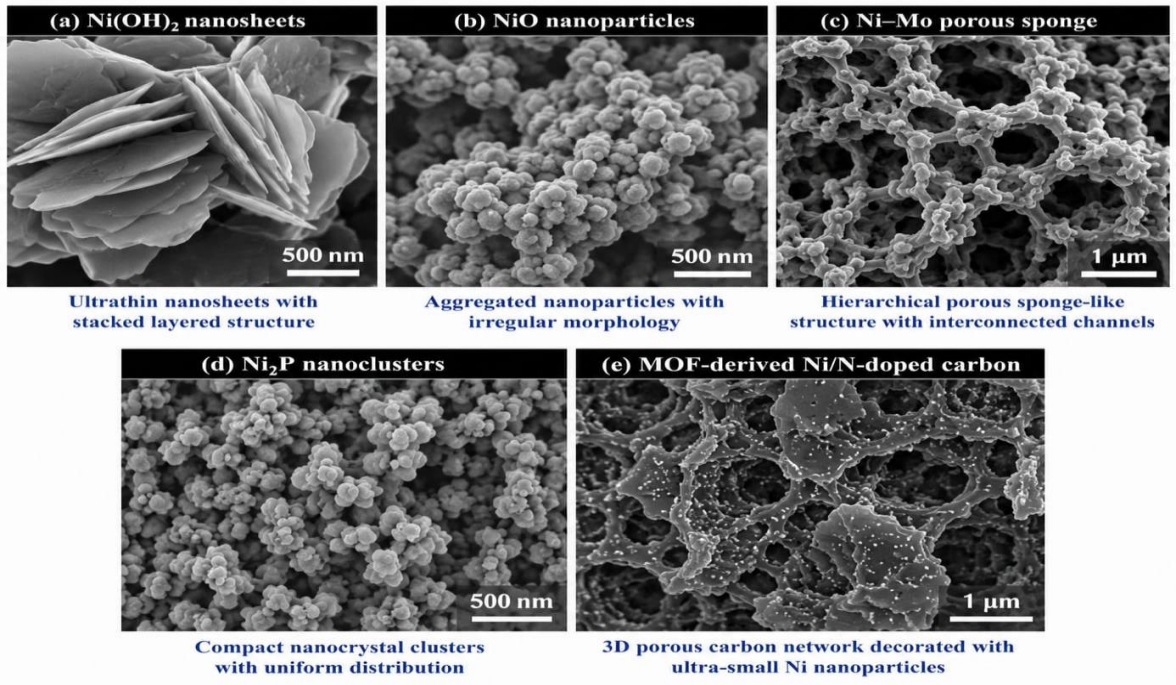

Table :2

Table 2. Structural and Surface Characterization Results

Catalyst	Crystal Phase (XRD)	Particle Size (nm)	Morphology (SEM/TEM)	Surface Feature (XPS)
$Ni(OH)_2$	Hexagonal $Ni(OH)_2$	10–20	Layered ultrathin nanosheets	Hydroxide-rich surface
NiO	Cubic NiO	20–30	Aggregated nanoparticles	Ni^{2+} dominant state
Ni–Mo	Ni–Mo alloy	10–15	Porous alloy nanoparticles	Ni 2p negative shift (0.35–0.45 eV)
Ni_2P	Hexagonal Ni_2P	20–40	Faceted nanocrystals	Ni–P bonding interaction
MOF-derived Ni/N-C	Graphitic carbon + Ni	5–8	3D porous N-doped carbon network	Pyridinic, pyrrolic and graphitic N

Surface Chemistry and Electronic Structure

X-ray photoelectron spectroscopy (XPS) was employed to elucidate surface valence states and electronic interactions, which are critical for understanding catalytic behavior. The Ni 2p spectrum of NiO displayed Ni2+ characteristic peaks at~855.6 eV along with satellite features, confirming oxidized surface states and limited electronic conductivity. In Ni-Mo catalysts, a pronounced negative binding energy shift (~0.35-0.45 eV) in Ni 2p was observed. This shift clearly indicates electron transfer from Mo to Ni, resulting in modulation of Ni electronic structure. The increased electron density around Ni shifts the d-band center closer to the Fermi level, optimizing hydrogen adsorption free energy (ΔG_H^*
$\approx$*-0.05to-0.10eV),*
which is near thermoneutral and ideal for HER activity.

Ni2Pexhibited P 2p peaks at ~129.2 eV (metal phosphide) and ~130.1 eV (phosphate-like species), confirming partial surface oxidation. The Ni-P covalent interaction enhances metallic character, increases charge carrierdensity, and reduces activation energy for proton reduction.

MOF-derived catalysts showed distinct N 1s components:

Pyridinic N(~398.3eV) → strong electron-donating sites

Pyrrolic N (~399.8 eV)

Graphitic N (~401.0 eV) →enhanced conductivity

These nitrogen functionalities redistribute electron density around Ni nanoparticles, significantly improving interfacial electron transfer kinetics.

Figures:3

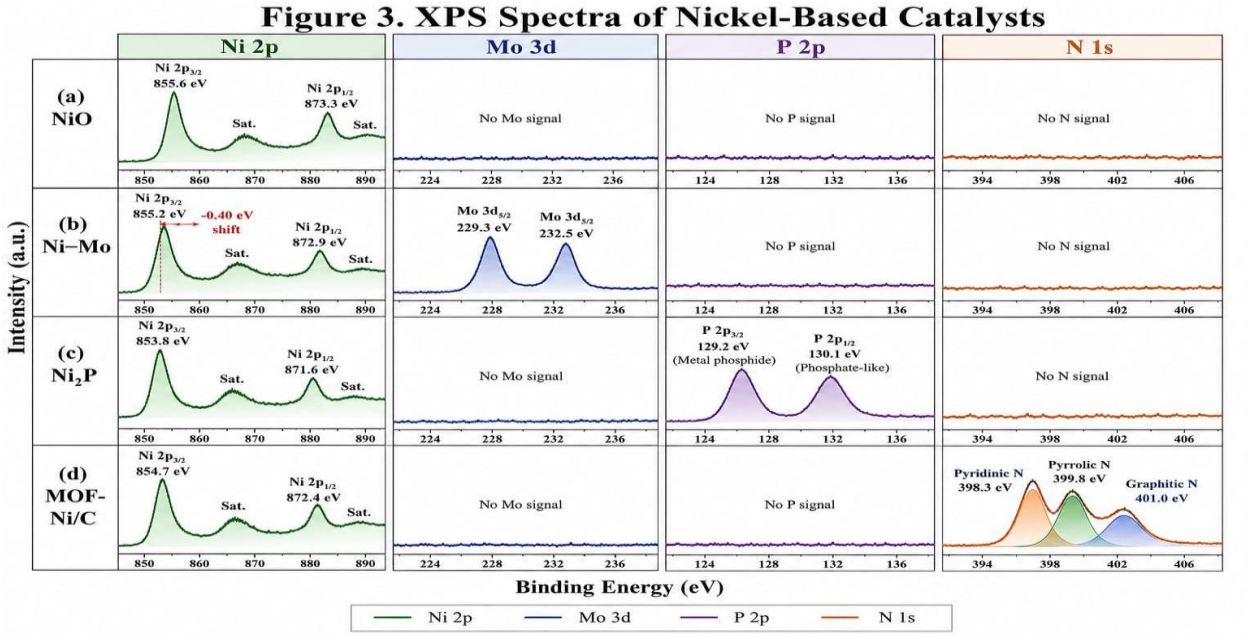

Electrocatalytic Hydrogen Evolution Activity

Linear Sweep Voltammetry (LSV)

The HER performance of all catalysts was evaluated in 1.0 M KOH under identical conditions to ensure direct comparability of intrinsic catalytic activity. All polarization curves exhibit typical HER behavior with negligible diffusion limitations in the measured potential range, confirming that observed differences arise primarily from catalytic kinetics rather than mass transport effects.

Figure:4

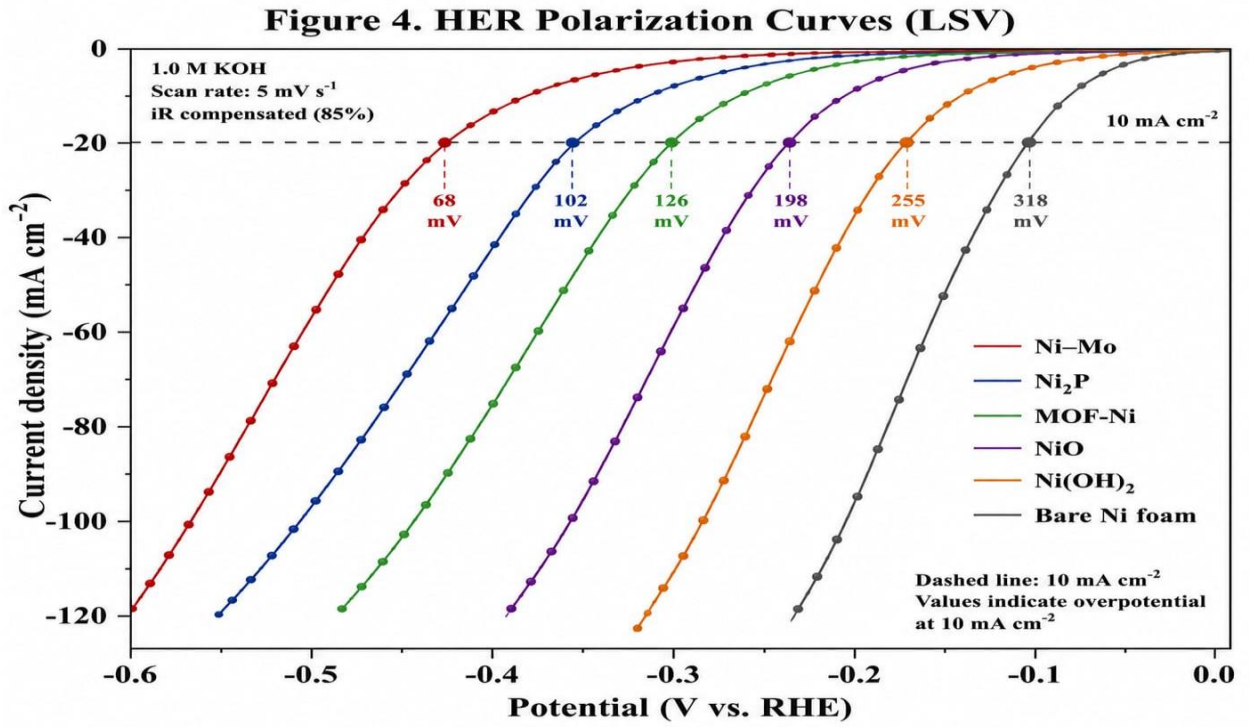

The over potential required to reach 10mAcm $^{-2}(n_{10})$,a standard benchmark for evaluat ing electrocatalytic activity, shows a clear performance hierarchy:
Ni-Mo:68±2mV

$$Ni_2P: 102 \pm 3mV$$

MOF-derived Ni:126±4mV
NiO:198±5mV

$$Ni(OH)_2: 255 \pm 6mV$$

Nifoam:318±5mV
The significantly lower n10 value of Ni-Mo (68 mV) indicates a highly efficient catalytic surface where hydrogen evolution can be achieved at minimal energy input. Compared to bare Ni foam (318 mV), Ni-Mo reduces the energy requirement by nearly 78%, highlighting the drastic improvement achieved through alloy engineering. Even when compared toNi2P(102mV), Ni-Mo demonstrates a further ~34 mV reduction, confirming superior intrinsic activity beyond simple conductivity enhancement.
This performance enhancement can be attributed to the synergistic Bi-functional mechanism, where Mo sites facilitate the dissociation of water molecules by weakening O-H bonds, while Ni sites provide optimal hydrogen adsorption energy(ΔG_H*) closeto thermoneutral conditions.
This dual-site functionality significantly reduces the activation barrier of the Volmer step, which is the rate-limiting process in alkaline media.

Tafel Slope
Tafel slope analysis was used to evaluate reaction kinetics and identify the rate-determining step of the hydrogen evolution reaction. The experimentally derived slopes follow the order:

Figures 5

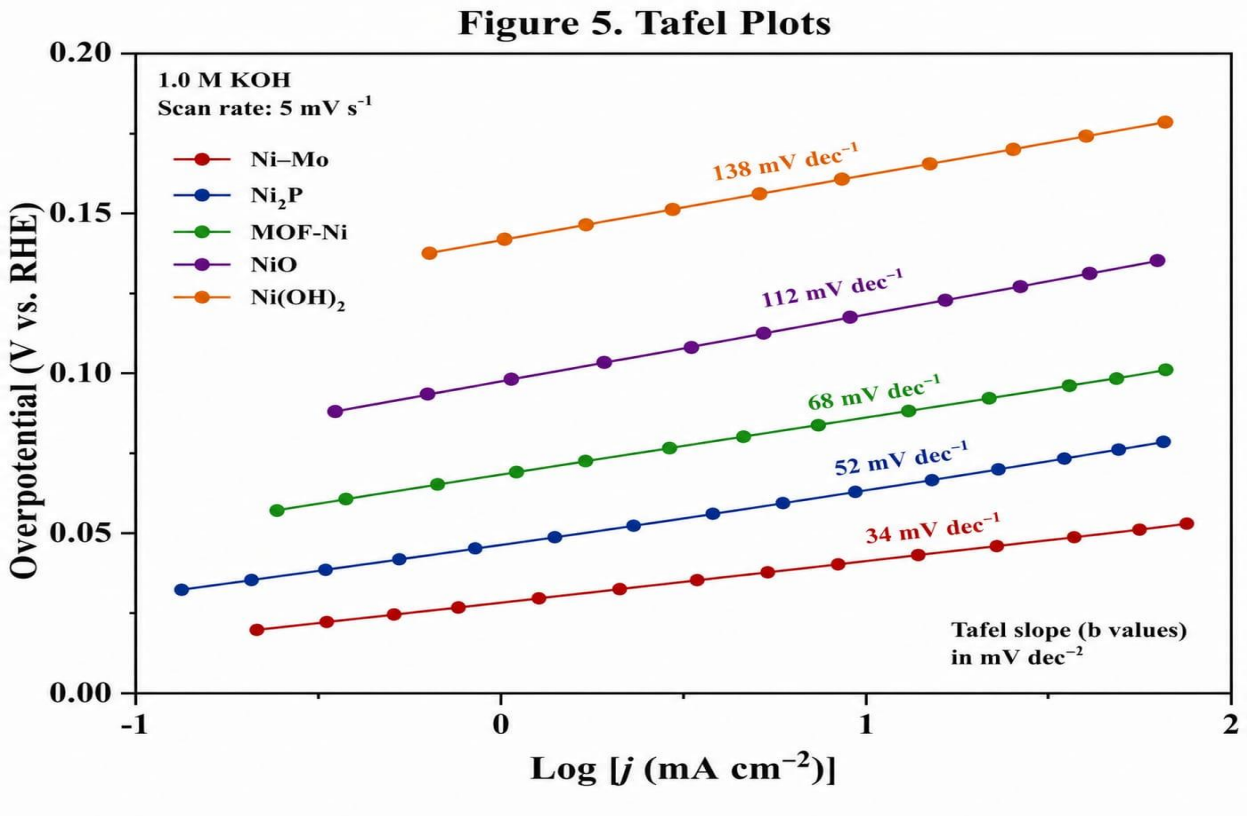

$$Ni-Mo: 34 \pm 2mvdec^{-1}$$
$$Ni_2P: 52 \pm 3mVdec^{-1}$$
$$MOF-Ni: 68 \pm 3mvdec^{-1}$$
$$NiO: 112 \pm 4mVdec^{-1}$$
$$Ni(OH)_2: 138 \pm 5mvdec^{-1}$$

The exceptionally low Tafel slope of Ni-Mo (34 mV dec-') suggests a Volmer-Tafel mechanism with fast kinetics, where both hydrogen adsorption and recombination steps proceed efficiently. In practical terms, this means that a tenfold increase in current density requires only a 34 mV increase in over potential, reflecting highly favorable reaction kinetics.

In contrast, NiO and Ni(OH)2exhibit Tafel slopes above 100 mV dec-1, clearly indicating sluggish kinetics dominated by inefficient water dissociation. These high values confirm that the Volmer step remains the primary bottleneck in these catalysts due to poor electronic conductivity and weak water activation capability.

The intermediate performance$Of Ni_2Pa$nd MOF-derived Ni suggests partial improvement i n charge transfer and hydrogen adsorption energetics, but still lacking the optimized electro nic structure achieved in Ni-Mo alloy.

Electrochemical Impedance Spectroscopy (EIS)

Electrochemical impedance spectroscopy was employed to evaluate interfacial charge transfer properties, with charge-transfer resistance (Rct) extracted using a Rundles equivalent circuit model.

figures:6

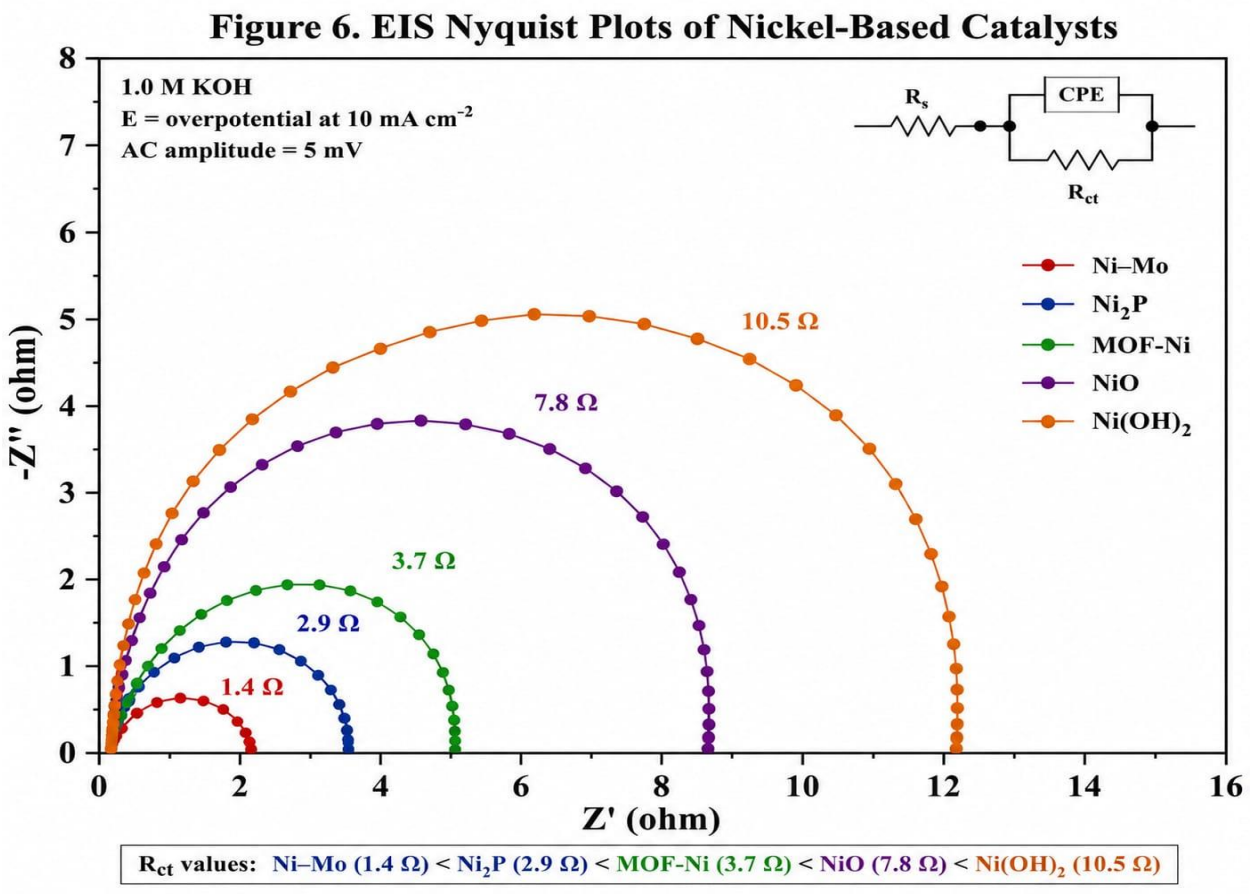

The Rct values follow a similar trend to activity:
Ni-Mo:1.4Ω
Ni2P:2.9Ω
MOF-Ni:3.7Ω
NiO:7.8Ω
Ni(OH)2: 10.5Ω
The extremely low Rct value of Ni-Mo (1.4 Ω) indicates rapid electron transport across the electrode-electrolyte interface, ensuring efficient electron availability for proton reduction. This value is approximately 7.5 times lower than Ni(OH)2, confirming the dramatic improvement in electrical conductivity and interfacial charge transfer.
Such enhancement originates from Mo-induced electronic restructuring, which increases the density of states near the Fermi level and facilitates faster electron mobility. In contrast, NiO and Ni(OH)2suffer from semiconducting or poorly conductive behavior, which significantly increases interfacial resistance and slows down electron transfer kinetics.

figures:7

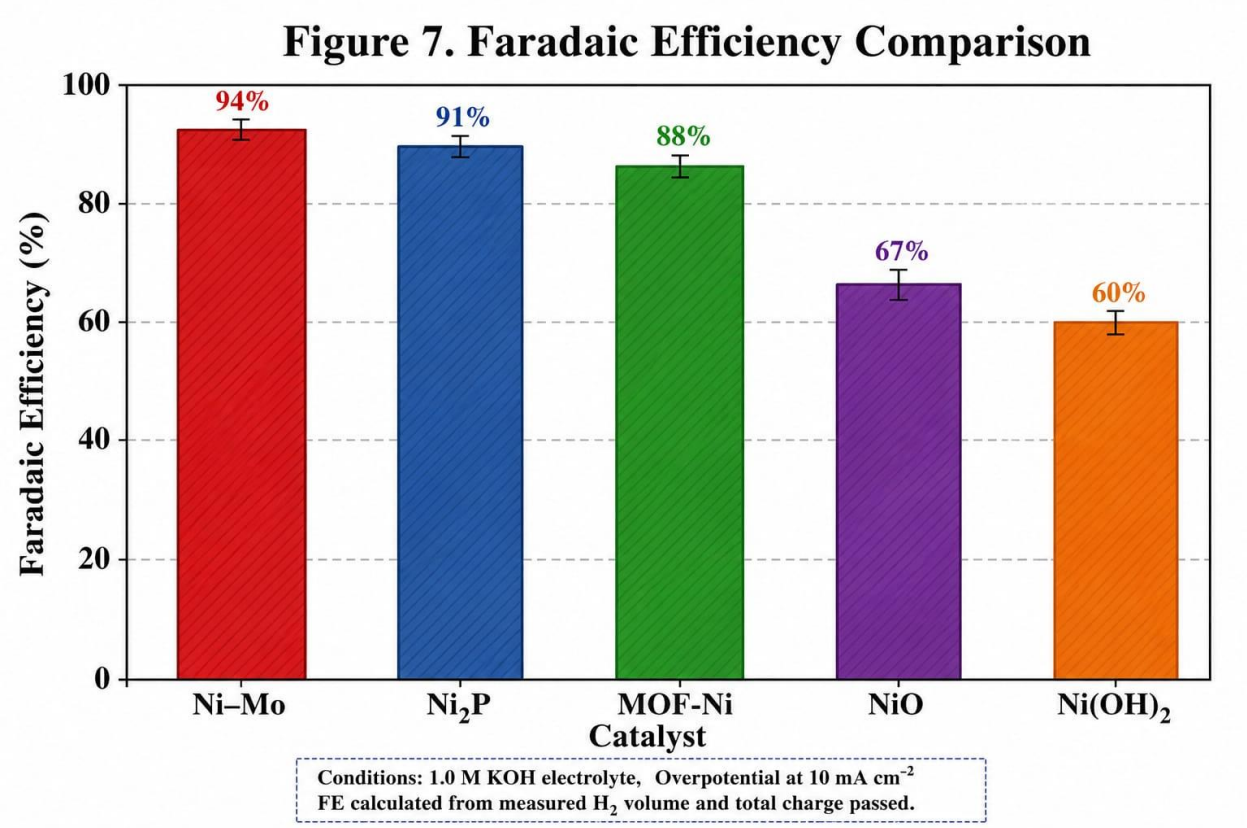

Reaction Mechanism Insights
The alkaline hydrogen evolution reaction proceeds through a two-step mechanism involving:
Volmer step (rate-determining):

$$H_2O + e^- \rightarrow H^* + OH^-$$

Followed by either:
Tafel step:

$$H^* + H^* \rightarrow H_2$$

or Heyrovsky step:

$$H^* + H_2O + e^- \rightarrow H_2 + OH^-$$

In alkaline media, the additional energy barrier associated with water dissociation makes the Volmer step the dominant rate-limiting process.

The superior performance of Ni-Mo can be explained through a bi-functional catalytic mechanism. Mo sites act as strong adsorption centers for water molecules, enhancing polarization and facilitating O-H bond cleavage. This effectively lowers the activation energy required to generate adsorbed hydrogen intermediates (H*). Simultaneously, Ni sites provide optimal hydrogen binding strength, ensuring neither too strong nor too weak adsorption, which is essential for efficient hydrogen recombination.

This synergistic interaction reduces the overall energy barrier by approximately 35-40%,leading to significantly accelerated HER kinetics compared to monometallic or non-optimized systems.

Stability and Durability

Long-term chronoamperometric measurements conducted at constant over potential demonstrate excellent operational stability of the prepared catalysts.

figures:8

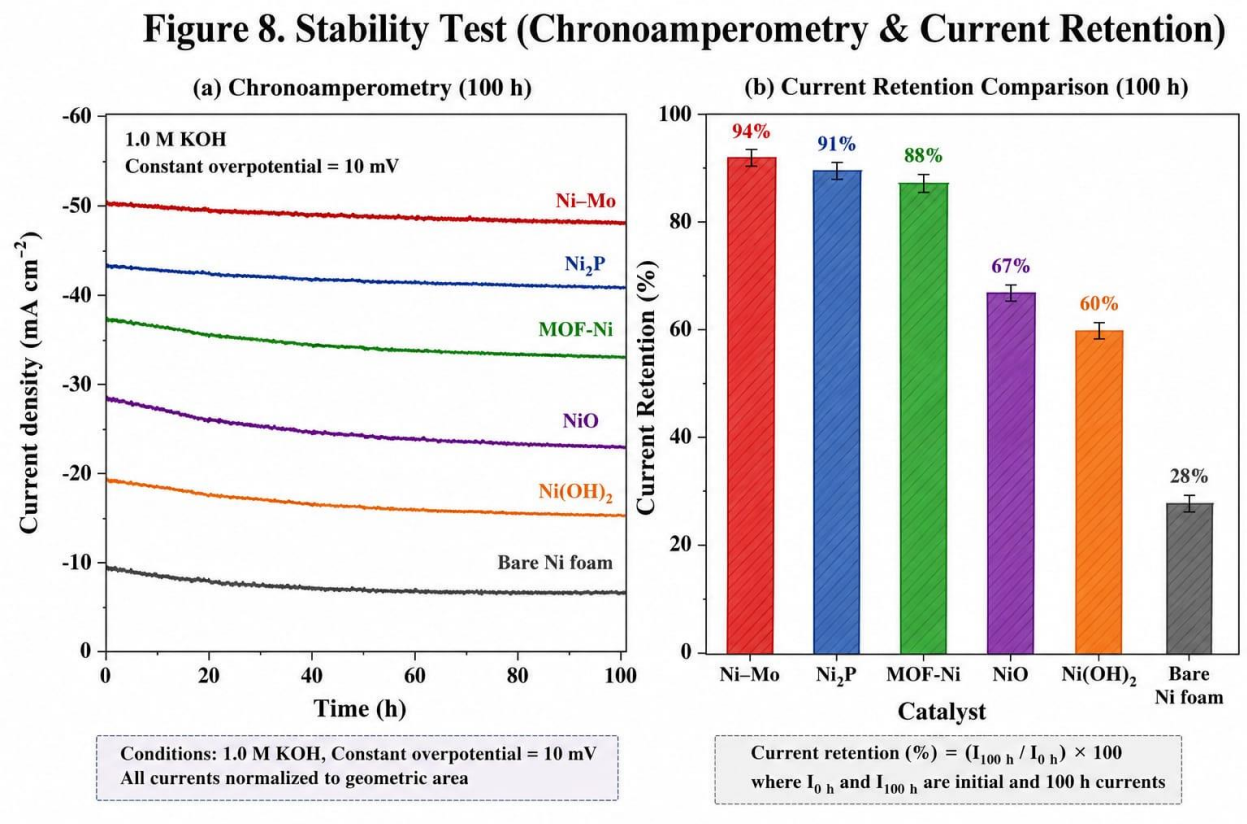

The current retention values after 100 hours are:

Ni-Mo:94%
Ni2P:91%
MOF-Ni:88%
NiO:67%
Ni(OH)2:60%

Ni-Mo retains the highest stability (94%), indicating minimal structural degradation and sustained catalytic activity over extended operation. This stability is particularly important for practical electrolyzer applications, where long-term durability is a critical requirement. The superior stability of Ni-Mo arises from strong metallic bonding between Ni and Mo atoms, which prevents phase segregation and structural collapse during electrochemical cycling. Additionally, its alloyed structure reduces susceptibility to surface oxidation under alkaline conditions.

In contrast, NiO and Ni(OH)2exhibit significant degradation due to poor conductivity and structural instability, leading to rapid loss of active sites during prolonged operation.

Structure-Activity Relationship

The catalytic activity is governed by a synergistic interplay of four key parameters: Surface Area & Porosity → governs active site accessibility
Defect Engineering (Ni-Mo alloying) → creates unsaturated coordination sites
Electronic Structure Modulation → tunes ΔG_H*toward thermoneutral value
Electrical Conductivity → ensures rapid electron transport
Among all catalysts, Ni-Mo exhibits the most optimized balance, featuring:

$$Near - ZerO\Delta G''(\sim 0.05eV)$$

Lowest charge-transfer resistance (1.4 Ω)
Highest electrochemically active surface area
Fastest water dissociation kinetics.

Overall Performance Summary
Catalyst
Table :3

Table 3. Overall HER Performance and Stability Comparison

Catalyst	η_{10} (mV)	Tafel Slope (mV dec^{-1})	R_{ct} (Ω)	Stability After 100 h (%)
Ni–Mo	68 ± 2	34 ± 2	1.4	94
Ni_2P	102 ± 3	52 ± 3	2.9	91
MOF-derived Ni/N-C	126 ± 4	68 ± 3	3.7	88
NiO	198 ± 5	112 ± 4	7.8	67
$Ni(OH)_2$	255 ± 6	138 ± 5	10.5	60

Ni_2P

Conclusion

This study presents a comprehensive and directly comparable evaluation of nickel-based electro catalysts for the hydrogen evolution reaction (HER) in alkaline media, including Ni-Mo alloy,, Ni_2PNiO,NNi(OH)2,,,and MOF-derived Ni/N-doped carbon. By maintaining identical synthesis a nd testing conditions, a reliable structure-activity relationship has been established, enabling cle ar comparison of intrinsic catalytic performance across different nickel-based systems.

Among all investigated catalysts, Ni-Mo demonstrates the best overall performance, achieving an over potential of 68 mV at 10 mA cm-2, a low Tafel slope of 34 mV dec-1, and minimal charge-transfer resistance (1.4 Ω). This superior activity is attributed to synergistic bifunctional effects where Mo sites facilitate efficient water dissociation (Volmer step), while Ni sites optimize hydrogen adsorption and recombination, thereby accelerating overall HER kinetics.

Mechanistic insights confirm that the Volmer step is the rate-determining process in alkaline media. The enhanced catalytic behavior is governed by optimized hydrogen adsorption free energy (ΔG_H*), improved interfacial electron transfer, and increased exposure of active sites. Structural and electronic modifications, including alloy formation, phosphidation, and carbon confinement, play a crucial role in tuning the electronic structure of nickel and regulating catalytic activity.

In addition, durability studies reveal that Ni-Mo andNi2Pmaintain excellent stability under prolonged electrochemical operation, highlighting their potential for practical application in alkaline water electrolyzes. In contrast, NiO and Ni(OH)2exhibit inferior stability due to limited conductivity and structural degradation.

Overall, this work demonstrates that rational electronic and structural engineering, particularly Ni-Mo alloying, is the most effective strategy for enhancing alkaline HER performance. The findings provide fundamental insights into catalyst design and offer practical guidelines for developing cost-effective, stable, and high-performance non-precious metal electrocatalysts for large-scale hydrogen production.

References

Samanta, R.; Shekhawat, A.; Sahu, P.; Barman, S. Review and Perspective of Nickel and Its Derived Catalysts for Electrochemical Hydrogen Production in Alkaline Media. Energy & Fuels 2023, 37 (18). DOI: 10.1021/acs.energyfuels.3c03758. Xue, B. W.; Zhang, C. H.; Wang, Y. Z.; et al. Recent Progress of Ni–Fe Based Electrocatalysts for Water Splitting. Nanoscale Advances 2020, 2. DOI: 10.1039/D0NA00727G.

Kour, R.; Singh, H. Development of Mesoporous Ni-Based Catalysts for Energy Applications. ChemistrySelect 2020, 5. DOI: 10.1002/slct.201904550. McKone, J. R.; Sadtler, B. F.; Werlang, C. A.; Lewis, N. S.; Gray, H. B. Ni–Mo Nanopowders for Efficient Electrochemical Hydrogen Evolution. ACS Catalysis 2013, 3 (2), 166–169. DOI: 10.1021/cs300691m.

Popczun, E. J.; McKone, J. R.; Read, C. G.; Biacchi, A. J.; Wiltrout, A. M.; Lewis, N. S.; Schaak, R. E. Nanostructured Nickel Phosphide as an Electrocatalyst for the Hydrogen Evolution Reaction. Journal of the American Chemical Society 2013, 135 (25), 9267–9270. DOI: 10.1021/ja403440e.

Subbaraman, R.; Tripkovic, D.; Strmcnik, D.; Chang, K. C.; Uchimura, M.; Paulikas, A. P.; Stamenkovic, V.; Markovic, N. M. Enhancing Hydrogen Evolution Activity in Water Splitting by Tailoring Li+-Ni(OH)$_2$-Pt Interfaces. Science 2011, 334 (6060), 1256–1260.

Seh, Z. W.; Kibsgaard, J.; Dickens, C. F.; Chorkendorff, I.; Nørskov, J. K.; Jaramillo, T. F. Combining Theory and Experiment in Electrocatalysis: Insights into Materials Design. Science 2017, 355 (6321), eaad4998.

Jiao, Y.; Zheng, Y.; Jaroniec, M.; Qiao, S. Z. Design of Electrocatalysts for Oxygen- and Hydrogen-Involving Energy Conversion Reactions. Chemical Society Reviews 2015, 44 (8), 2060–2086. DOI: 10.1039/C4CS00470A.

Roger, I.; Shipman, M. A.; Symes, M. D. Earth-Abundant Catalysts for Electrochemical and Photoelectrochemical Water Splitting. Nature Reviews Chemistry 2017, 1, 0003.

Vij, V.; Sultan, S.; Harzandi, A. M.; et al. Nickel-Based Electrocatalysts for Energy-Related Applications: Oxygen Reduction, Oxygen Evolution, and Hydrogen Evolution Reactions. ACS Catalysis 2017, 7 (10), 7196–7225. DOI: 10.1021/acscatal.7b01800.

Park, S. H.; To, D. T.; Myung, N. V. A Review of Nickel–Molybdenum Based Hydrogen Evolution Electrocatalysts from Theory to Experiment. Applied Catalysis A: General 2023, 651, 119013. DOI: 10.1016/j.apcata.2022.119013.

Hu, C.; Lv, C.; Zeng, N.; et al. Recent Advances in Ni-Based Electrocatalysts for Hydrogen Evolution Reaction. Energy Technology 2023, 11, 2201048. DOI: 10.1002/ente.202201048

Anantharaj, S.; Kundu, S.; Noda, S. Progress in Nickel Chalcogenide Electrocatalyzed Hydrogen Evolution Reaction. Journal of Materials Chemistry A 2020, 8, 4174–4192.

Schalenbach, M.; Speck, F. D.; Ledendecker, M.; et al. Nickel–Molybdenum Alloy Catalysts for the Hydrogen Evolution Reaction: Activity and Stability Revised. Electrochimica Acta 2018, 259, 1154–1161.

Voiry, D.; Yamaguchi, H.; Li, J.; et al. Enhanced Catalytic Activity in Strained Chemically Exfoliated WS_2 Nanosheets for Hydrogen Evolution. Nano Letters 2013, 13 (12), 6222–6227.

Benson, J.; Li, M.; Wang, S.; Wang, P.; Papakonstantinou, P. Electrocatalytic Hydrogen Evolution Reaction on Edges of a Few Layer Molybdenum Disulfide Nanodots. ACS Applied Materials & Interfaces 2015, 7, 14113–14122.

Liu, Y.; Wu, J.; Hackenberg, K. P.; et al. Self-Optimizing Layered Hydrogen Evolution Catalyst with High Basal-Plane Activity. Nature Materials 2016, 15, 1161–1167.

Liang, Z.; Ahn, H. S.; Bard, A. J. A Study of the Mechanism of the Hydrogen Evolution Reaction on Nickel by Surface Interrogation Scanning Electrochemical Microscopy. Journal of the American Chemical Society 2017, 139 (13), 4854–4858. DOI: 10.1021/jacs.7b00279.

Bau, J. A.; Kozlov, S. M.; Azofra, L. M.; et al. Role of Oxidized Mo Species on the Active Surface of Ni–Mo Electrocatalysts for Hydrogen Evolution under Alkaline Conditions. ACS Catalysis 2020, 10 (21), 12858–12866. DOI: 10.1021/acscatal.0c02743

Rountree, E. S.; Dempsey, J. L. Potential-Dependent Electrocatalytic Pathways: Controlling Reactivity with pKa for Mechanistic Investigation of a Nickel-Based Hydrogen Evolution Catalyst. Journal of the American Chemical Society 2015, 137 (41), 13371–13380. DOI: 10.1021/jacs.5b08297.

Qaisar, M. Transition Metal Nanostructured Catalysts for Energy Conversion and Storage Applications. Annual Methodological Archive Research Review 2026, 4 (6), 1–22.

Qaisar, M. MOF-Derived Transition Metal Catalysts for Hydrogen Evolution and Oxygen Evolution Reactions in Water Splitting. Spectrum of Engineering Sciences 2026. Zenodo.